Vpliv pravokotnosti mreže na konvergenco programa SIMPLE za reševanje Navier-Stokes-ovih enačb

The Influence of Grid Orthogonality on the Convergence of the SIMPLE Algorithm for Solving Navier-Stokes Equations

Ivo Džijan - Zdravko Virag - Hrvoje Kozmar
(University of Zagreb, Croatia)

Razvili smo metodo končnih volumnov za reševanje Navier-Stokesovih enačb na lokalno pravokotni nestrukturirani mreži z uporabo algoritma SIMPLE. Razvito metodo smo primerjali s podobno metodo na strukturirani, ne nujno pravokotni mreži, v členih pretekle konvergence in obsegu pod-relaksacijskih faktorjev, pri katerih se metodi približujeta. Kadar je strukturirana mreža pravokotna, sta stopnji približevanja obeh metod podobni. V primerih, kadar strukturirana mreža ni pravokotna, se pokaže prednost predlagane metode pri lokalno pravokotni mreži v razmerah pretekle konvergence. V teh primerih je obseg pod-relaksacijskih faktorjev, pri katerih je predlagana metoda zadovoljivo konvergentna, mnogo večji kot pri metodi na nepravokotni mreži.
(Ključne besede: Navier-Stokesove enačbe, metode končnih volumnov, algoritmi SIMPLE, nestrukturirane mreže)

A finite-volume method for solving the Navier-Stokes equations on a locally orthogonal unstructured grid using the SIMPLE algorithm has been developed. The developed method was compared with a similar method on a structured, not necessarily orthogonal grid, in terms of convergence history and the range of under-relaxation factors in which the methods converge. When the structured grid is orthogonal, the convergence rates of the two methods are similar. For the cases when the structured grid is non-orthogonal, the superiority of the proposed method on the locally orthogonal grid is demonstrated in terms of convergence history. In these cases, the range of under-relaxation factors in which the proposed method shows satisfactory convergence is much wider than for the method on the non-orthogonal grid.
(Keywords: Navier-Stokes equations, finite volume methods, SIMPLE algorithm, unstructured grid)

0 INTRODUCTION

The rapid development of computers has brought about rapid developments in the field of computational fluid dynamics. Calculation domains are now more complex, which increases the need to use an unstructured grid for their discretization. Finite volume methods are widely applied for solving fluid flow problems. Initially, these methods were used on structured staggered grids. Nowadays they are used on unstructured collocated grids, on which segregate algorithms with the pressure-based approach are applied for incompressible flows. The most popular algorithm based on pressure correction is the SIMPLE (Semi-Implicit Method for the Pressure-Linked Equation) algorithm, Caretto et al. [1] and Patankar and Spalding [2]. In the pressure-velocity correction relation the effects coming from velocity corrections in neighboring nodes on the pressure correction in the central node are neglected. The consequence of this neglecting is the overestimation of the pressure correction, which can cause the divergence of the numerical process. To ensure the stability of the numerical process, the under-relaxation factor for the pressure is introduced. The optimal value of this factor cannot be estimated in advance since it depends on the grid's characteristics and the nature of the problem.

The SIMPLE algorithm is originally defined on a staggered grid where the pressure is calculated

in the cell centre and the velocity components are calculated on the cell faces. On a collocated grid, the pressure field and velocity components are calculated in the cell centre. The application of the SIMPLE algorithm on a collocated grid started with Rhie and Chow [3].

The grid non-orthogonality is one of the factors that increases the number of iterations of the SIMPLE algorithm. If the connecting line of two neighboring nodes is not perpendicular to the cell face, some terms that appear due to non-orthogonality are usually neglected. This is the case with the CAFFA public-domain computer code [4]. It is believed that this neglecting slows down the rate of convergence of the numerical method. Therefore, the modification of the finite volume method on an unstructured locally orthogonal grid is proposed. The rate of convergence of the SIMPLE algorithm on that grid will be compared with the rate of convergence on a structured, not necessarily orthogonal grid.

1 MATHEMATICAL MODEL AND NUMERICAL PROCEDURE

The mathematical model of steady, laminar, incompressible fluid flow with constant viscosity and without mass forces is adopted. The model is described with the following Navier-Stokes equations:

$$\frac{\partial}{\partial x_j}\left(\rho v_j\right) = 0 \tag{1}$$

$$\frac{\partial}{\partial x_j}\left(\rho v_j v_i\right) = -\frac{\partial p}{\partial x_i} + \mu \frac{\partial^2 v_i}{\partial x_j \partial x_j} \tag{2}$$
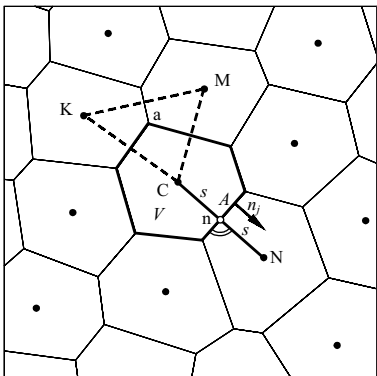

Fig. 1. *A part of calculation domain and a typical cell of locally-orthogonal unstructured grid*

where ρ, v_j, p, μ and x_j are the fluid density, velocity, pressure, viscosity and coordinates, respectively. These equations will be numerically solved on an unstructured locally orthogonal grid. A part of such a computational grid is shown in Fig. 1.

The main nodes, C and N, at which the velocity and pressure fields are calculated, are placed within their respective cells. The connecting line CN is perpendicular to the cell face and the nodes C and N are at an equal distance from an auxiliary node n, which enables a simple formulation of the high-order interpolation. It is clear that such a grid is possible in every 2D case, because the cell vertex a in Fig. 1 is the circumcenter of the triangle formed by the nodes C, M and K. Such a grid generator is described by Džijan [5], which includes a grid-smoothing procedure that forces the main nodes to be close to the cell centroids and the auxiliary nodes to be close to the cell-face centroids.

Discretization of the equations starts with integrating over the cell volume V, according to Fig. 1. By using the Gauss theorem and the mean-value theorem, the integrated governing equations take the form:

$$\sum_{k=1}^{m}\left[F\right]^k = 0 \tag{3}$$

$$\sum_{k=1}^{m}\left[F v_i\big|_n - \mu A \frac{\partial v_i}{\partial x_j}\bigg|_n n_j\right]^k = -V \frac{\partial p}{\partial x_i}\bigg|_C + \sum_{k=1}^{m}\left[\mu A \frac{\partial v_j}{\partial x_i}\bigg|_n n_j\right]^k \tag{4}$$

where $F = \rho A v_j\big|_n n_j = \rho A v_n$ is the mass flow through the cell face and $J_i = F v_i\big|_n - \mu A (\partial v_i / \partial x_j)\big|_n n_j$ is the momentum flux through the cell face. A and n_j are the cell-face area and its outward normal vector, V is the cell volume, while k denotes the cell-face index and m is the number of cell faces on the considered volume. The scope of the differencing schemes is to define the velocity $v_i\big|_n$ and its normal derivatives at the auxiliary node n in terms of velocity values at the main nodes. Since the adopted grid is locally orthogonal, these values are defined by using only the values at nodes C and N. A blending scheme of the central differencing scheme (CDS) and of the first-order upwind differencing scheme (UDS) is used in the CAFFA computer code. Therefore, the same scheme will also be used in the proposed method. In the case of the locally orthogonal grid, the diffusion part of the flux vector is modeled with the following equation:

$$J_i^d = -\mu A \frac{\partial v_i}{\partial x_j}\bigg|_n n_j = -\mu A \frac{\partial v_i}{\partial n}\bigg|_n = -\mu A \frac{v_i\big|_N - v_i\big|_C}{2s} \tag{5}.$$

In the case of a non-orthogonal grid, an additional term appears. In the CAFFA computer code this term is implemented by using the deferred correction approach, i.e., by using the velocity values from the previous iteration.

In the first-order UDS, the convective flux is modelled by:

$$J_i^{UDS} = F v_i \big|_n = \begin{cases} F v_i \big|_C & \text{for } F>0 \\ F v_i \big|_N & \text{for } F<0 \end{cases} \qquad (6),$$

and in the CDS (for the case when the node n lies in the middle of the CN connection line) by:

$$J_i^{CDS} = \frac{1}{2} F \left(v_i \big|_C + v_i \big|_N \right) \qquad (7).$$

By introducing the mixing factor γ, the final expression for the momentum flux is:

$$J_i = (1-\gamma) J_i^{UDS} + \gamma J_i^{CDS} + J_i^d \qquad (8)$$

where, for $\gamma = 0$ the result is the UDS, and for $\gamma = 1$ the CDS.

Introducing the expressions for the fluxes into (4) results in:

$$a_C v_i \big|_C - \sum_{k=1}^m \left[a_N v_i \big|_N \right]^k = -V \frac{\partial p}{\partial x_i}\bigg|_C + b_i \qquad (9)$$

where:

$$a_N = \left[\max(-F, 0) + \frac{\mu A}{2s} \right] \qquad (10),$$

$$a_C = \sum_{k=1}^m \left[a_N \right]^k \qquad (11)$$

and

$$b_i = \gamma \left\{ \sum_{k=1}^m \left[\frac{1}{2} F v_i \big|_N \right]^k - \sum_{k=1}^m \left[\max(-F,0) \right]^k v_i \big|_C + \sum_{k=1}^m \left[\max(-F,0) v_i \big|_N \right]^k \right\} \qquad (12).$$

It is obvious that all the terms coming from the CDS are treated as a deferred correction, the same as in the CAFFA code.

To reduce the possibility that the numerical process diverges, this equation is under-relaxed in the following form:

$$\left(1 + \frac{1}{\alpha_{uv}}\right) a_C v_i \big|_C - \sum_{k=1}^m \left[a_N v_i \big|_N \right]^k = -V \frac{\partial p}{\partial x_i}\bigg|_C + b_i + \frac{a_C v_i \big|_C}{\alpha_{uv}} \qquad (13)$$

which was proposed by Patankar [6]. The last term on the right-hand side is calculated from the previous iteration, and α_{uv} is the under-relaxation factor for the velocity.

According to Rhie and Chow [3], the mass flow through the cell face is defined as follows:

$$F = \rho A v_n = \rho A \overline{(v_n)} - \rho A \overline{\left(\frac{V_n}{a_n}\right)} \left[\frac{\partial p}{\partial n}\bigg|_n - \overline{\left(\frac{\partial p}{\partial n}\bigg|_n\right)} \right] \qquad (14)$$

where the line above a symbol indicates the linear interpolation between the values at nodes C and N, as follows:

$$\overline{(v_n)} = \frac{1}{2}\left(v_j\big|_C + v_j\big|_N\right) n_j \qquad (15),$$

$$\overline{\left(\frac{\partial p}{\partial n}\bigg|_n\right)} = \frac{1}{2}\left(\frac{\partial p}{\partial n}\bigg|_C + \frac{\partial p}{\partial n}\bigg|_N\right) \qquad (16)$$

and

$$\overline{\left(\frac{V_n}{a_n}\right)} = \frac{1}{2}\left(\frac{V_C}{(a_C)\big|_C} + \frac{V_N}{(a_C)\big|_N}\right) \qquad (17).$$

In the case of a locally orthogonal grid, the normal derivative of the pressure is defined by using the CDS, as follows:

$$\frac{\partial p}{\partial n}\bigg|_n = \frac{p_N - p_C}{2s} \qquad (18).$$

In the CAFFA code, where the grid is non-orthogonal, additional terms emerge and are treated explicitly by using the values from the previous iteration.

Solving the momentum equation with a given pressure field p^* results in the velocity field v_i^*, and the mass flow F^*, which does not necessarily satisfy the continuity equation. For that reason, the velocity corrections v_i' and the corresponding F' and pressure correction p' are searched, so that the corrected velocity field $v_i = v_i^* + v_i'$ and corrected mass flow $F = F^* + F'$ satisfy the continuity equation. According to Equation (14), the corrected mass flow is approximated as follows:

$$F = F^* - \frac{\rho A}{2s}\left(\frac{V_n}{a_n}\right)(p_N' - p_C') = F^* - a_N^{p'}(p_N' - p_C') \qquad (19).$$

Introducing the corrected mass flows in the continuity equation (3) results in the following equation for the pressure correction:

$$a_C^{p'} p_C' - \sum_{k=1}^m \left[a_N^{p'} p_N' \right]^k = b^{p'} \qquad (20)$$

where

$$a_C^{p'} = \sum_{k=1}^m \left[a_N^{p'} \right]^k \qquad (21)$$

and

$$b^{p'} = -\sum_{k=1}^m \left[F^* \right]^k \qquad (22).$$

The solving of this equation results in the pressure-correction field. Therefore, the pressure

field is corrected using the following equation:

$$p_C = p_C^* + \alpha_p p_C' \qquad (23)$$

where α_p is the under-relaxation factor for the pressure. The velocities in the main nodes are corrected as follows:

$$v_i|_C = v_i^*|_C - \frac{V}{a_C}\frac{\partial p'}{\partial x_i}\bigg|_C \qquad (24).$$

The gradients of the physical values in the main nodes are calculated using the Gauss formula as follows:

$$\frac{\partial \phi}{\partial x_i}\bigg|_C = \frac{1}{V}\sum_{k=1}^{m}[\phi_n n_i A]^k = \frac{1}{2V}\sum_{k=1}^{m}[\phi_N n_i A]^k \qquad (25)$$

where ϕ can stand for v_i, p or p'.

The steps in the SIMPLE algorithm for solving the Navier-Stokes equations can be summarized as follows:

1. Guess the pressure field p^* and the velocity field v_i.
2. Solve the momentum equation (13) to obtain v_i^*.
3. Solve the p' equation (20). Correct the pressure according to (23), correct the velocity according to (24) and the mass flow according to (19).
4. Treat the corrected pressure as p^* and return to Step 2. Repeat the whole procedure until a converged solution is obtained.

The converged solution is obtained when the normalized residuals for the continuity and momentum equations become smaller than some small number, ε. In this paper $\varepsilon = 10^{-6}$ was used. The residual for the continuity equation is:

$$R_m = \sum_{l=1}^{M}\left[\left|b^{p'}\right|\right]^l \qquad (26)$$

and the residual for the momentum is:

$$R_{v_i} = \sum_{l=1}^{M}\left[\left|a_C v_i|_C - \sum_{k=1}^{m}\left[a_N v_i|_N\right]^k + V\frac{\partial p}{\partial x_i}\bigg|_C - b_i\right|\right]^l \qquad (27).$$

In the above expressions, l denotes the cell index and M the total number of cells. The values of the variables in the above formula are from the current iteration, and the coefficients are prepared for the next iteration. The following residuals are usually normalized: the mass residuals with the inlet mass-flow rate and the residuals for the momentum equation with the inlet momentum flow rate.

2 RESULTS

The described numerical method is implemented in the FVM computer code. In this code the residuals are defined and normalized in the same way as in the CAFFA code. The rate of convergence of the described method and of the method used in the CAFFA code will be compared by varying the grid's non-orthogonality and the differencing scheme. Also, the range of under-relaxation factors in which the numerical procedure converges will be analyzed.

2.1 Laminar flow in a lid-driven cavity with inclined side walls

In this test the 2D laminar fluid flow is calculated in a closed cavity whose lid is moving in a tangential direction with velocity v_t Perić [7]. The Reynolds number based on the side length a is Re $= \rho.v_t.a/\mu = 1000$. The calculation is performed for different inclination angles of the side walls, $\beta = 90°$, $67.5°$ and $45°$. In this problem the residuals defined by (26) and (27) are not normalized.

Fig. 2 shows the qualitative picture of the streamlines for $\beta = 90°$ and $45°$. It is obvious that the initially assumed constant-velocity field will be very different from the final solution.

The problem is solved using the CAFFA numerical code on structured grids of size 40x40 cells, and with the FVM code on unstructured grids with approximately 1600 cells. Fig. 3 a shows a part of the unstructured grid for $\beta = 45°$ that is used in the FVM code. The borders of the finite volumes are presented, and the main nodes are marked. Fig. 3 b shows a part of the geometric grid for the same case, which is used in the CAFFA code. The displayed lines connect the main nodes at which the pressure and velocity fields are calculated.

In the SIMPLE algorithm, two under-relaxation factors should be given. The rate of convergence depends on the values of these two factors. Their optimal values are not known in advance, so that the described problem will be solved for a range of under-relaxation factors by varying α_{uv} from 0.5 to 0.95 with a step of 0.025, and α_p from 0.1 to 0.6 with a step of 0.1. The comparison criteria will be the number of iterations needed for the residuals to fall below $\varepsilon = 10^{-6}$.

In the CAFFA and FVM codes different solvers for linear algebraic equations are used. For this reason, a sufficient number of inner iterations is given at every iterative step to be sure that the systems are solved equally well in both codes.

Fig. 4 shows the numbers of outer iterations N_ε required to reduce the residual levels to ε as a function of the under-relaxation factors α_{uv} and α_p,
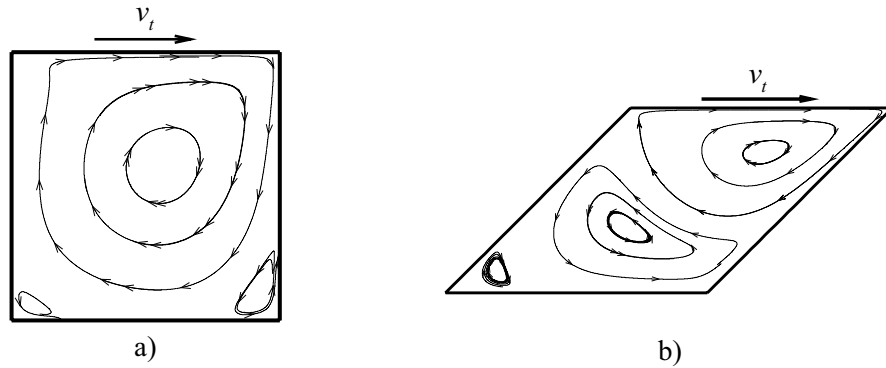
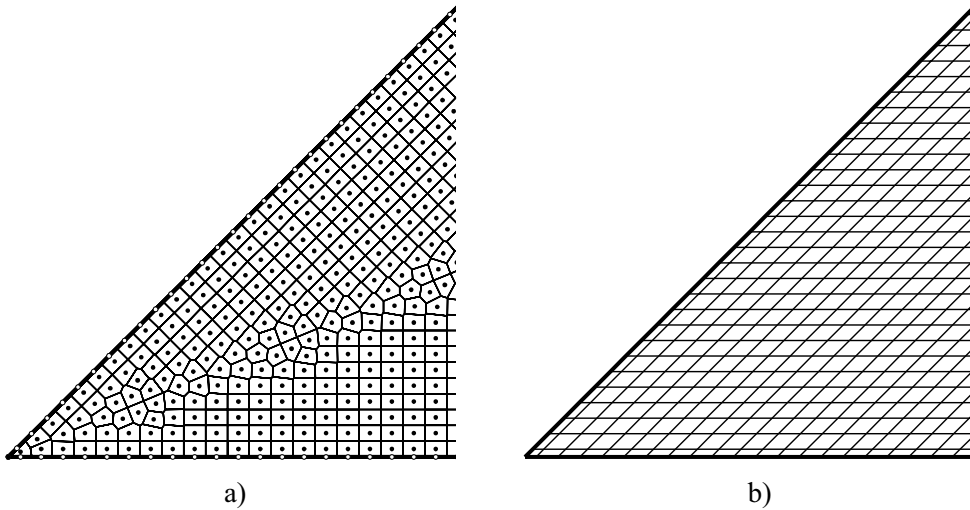Fig. 2. *Streamlines in laminar flow in a lid-driven cavity a) $\beta = 90°$, b) $\beta = 45°$*

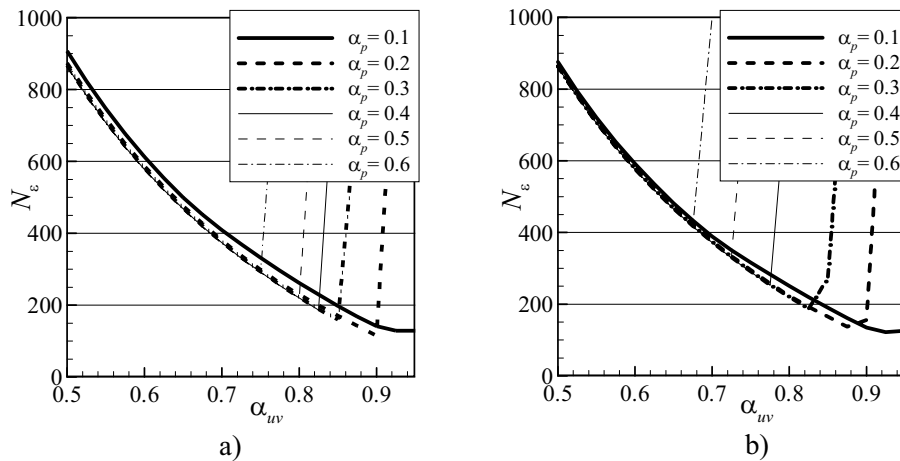Fig. 3. *A part of the grid for the lid-driven cavity problem for $\beta = 45°$ a) FVM, b) CAFFA*

Fig. 4. *Required number of outer iterations to reduce residual levels to $\varepsilon = 10^{-6}$ for the lid-driven cavity problem for $\beta = 90°$ (UDS) a) FVM, b) CAFFA*

for $\beta = 90°$. In this case, the grids for both codes are orthogonal, and the achieved results are almost identical. This confirms the equivalent implementation of the SIMPLE algorithm in both codes.

Fig. 5 shows N_ε for two algorithms for $\beta = 45°$. The SIMPLE algorithm in the CAFFA code converges in that situation only in the case that $\alpha_p = 0.1$, and only for small $\alpha_{uv} \leq 0.7$. N_ε is considerably
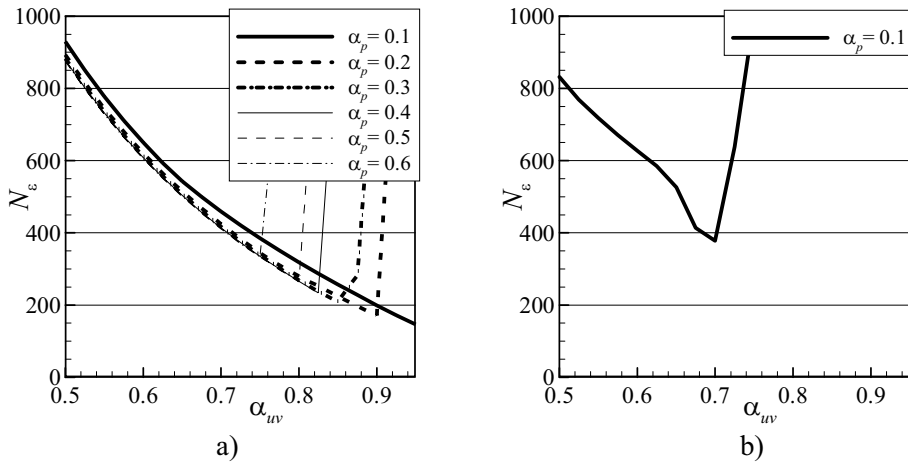
Fig. 5. *Number of outer iterations required to reduce the residual levels to ε = 10⁻⁶ for the lid-driven cavity problem for β = 45° (UDS) a) FVM, b) CAFFA*

larger than for the FVM code, which is a consequence of the grid's non-orthogonality.

Fig. 6 shows N_ε for two algorithms for $\beta = 67.5°$. In the FVM code, the necessary number of iterations has not significantly changed compared with the two previous cases. In the CAFFA code, the range of under-relaxation factors in which the algorithm converges is narrower than for $\beta = 90°$, and wider than for $\beta = 45°$. For the same combination of under-relaxation factors, N_ε increases with the increase of the grid's non-orthogonality.

Fig. 7 a shows the convergence histories (the greatest of three residuals versus the number of iterations N_{it}) of two methods for $\beta = 90°$, 67.5° and 45°, at a corresponding optimum combination of under-relaxation factors and by using the UDS. It is obvious that the convergence history on a locally

orthogonal grid is unaffected by β, unlike the case of a non-orthogonal grid. It is worth noting that this comparison is valid for optimum values of under-relaxation factors that are unknown prior to the calculation. The clear advantage of the locally orthogonal grid over the non-orthogonal one can be read from Figs 4 to 6, from which one can conclude that the convergence history on this grid is slightly changed by a relatively large deviation from the optimum combination of under-relaxation factors, which is not the case for the non-orthogonal grid.

Fig. 7 b shows the convergence histories of two methods for $\beta = 90°$ and 45°, at a corresponding optimum combination of under-relaxation factors and by using the CDS. The optimum values of the under-relaxation factors are the same as for the UDS. The rate of convergence slows down by switching from
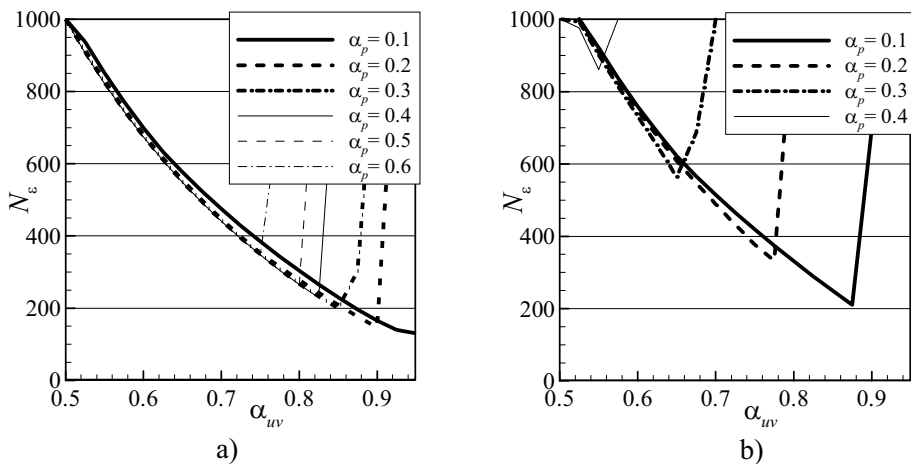

Fig. 6. *Number of outer iterations required to reduce the residual levels to ε = 10⁻⁶ for the lid-driven cavity problem for β = 67.5° (UDS) a) FVM, b) CAFFA*
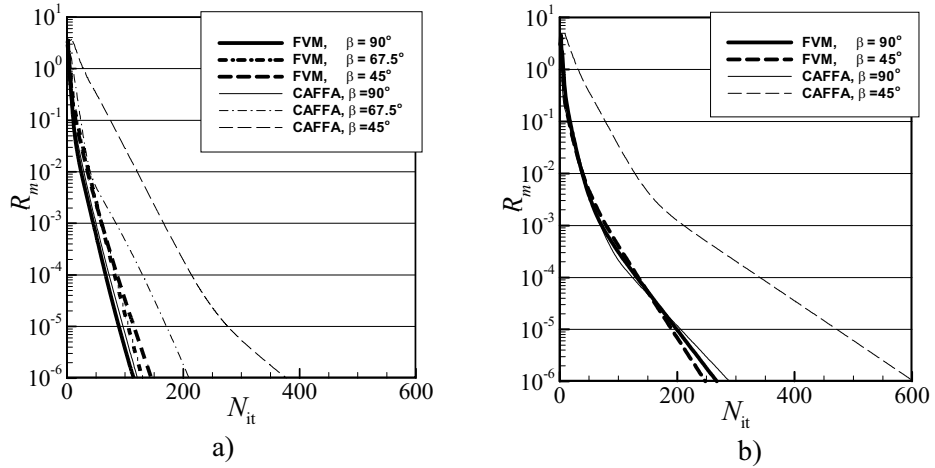
Fig. 7. *Convergence histories for the SIMPLE algorithm in the FVM and CAFFA codes for the lid-driven cavity problems a) UDS, b) CDS scheme*

the UDS to the CDS, which can be explained with the implementation of the CDS by using the deferred correction approach. Again, for $\beta = 90°$ the convergence history of the two methods is practically the same. For $\beta = 45°$ the convergence history of the method on a non-orthogonal grid is considerably slowed down due to the addition of the deferred correction on the non-orthogonality effects.

2.2 Laminar flow in a curved channel

The example of laminar flow in a curved channel where the grid is in some parts orthogonal and in some parts non-orthogonal is chosen. This is the usual case in practical applications of this method.
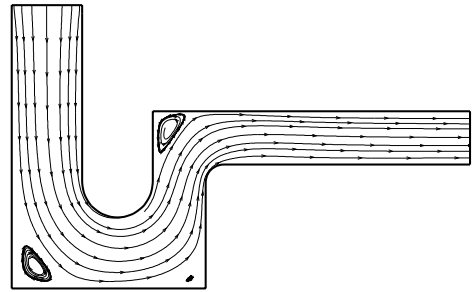

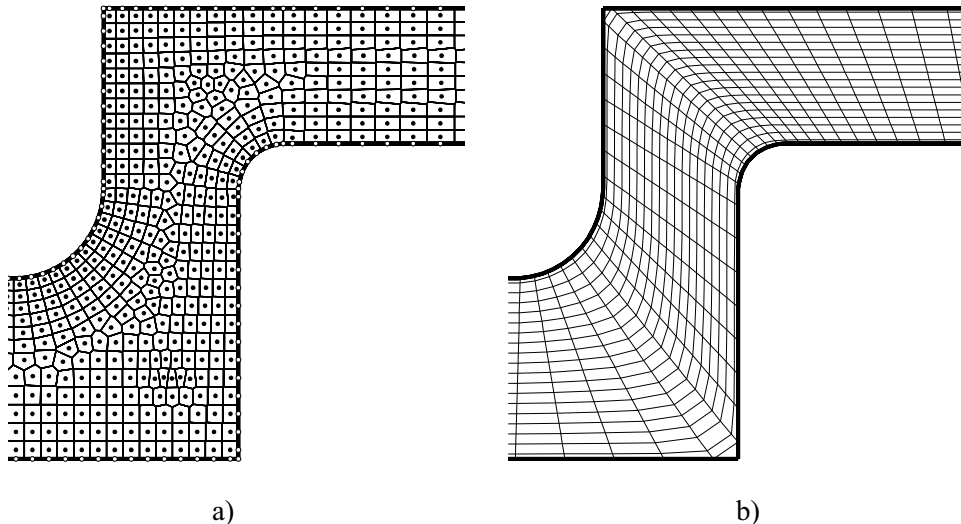Fig. 8. *Streamlines for laminar flow in a curved channel*

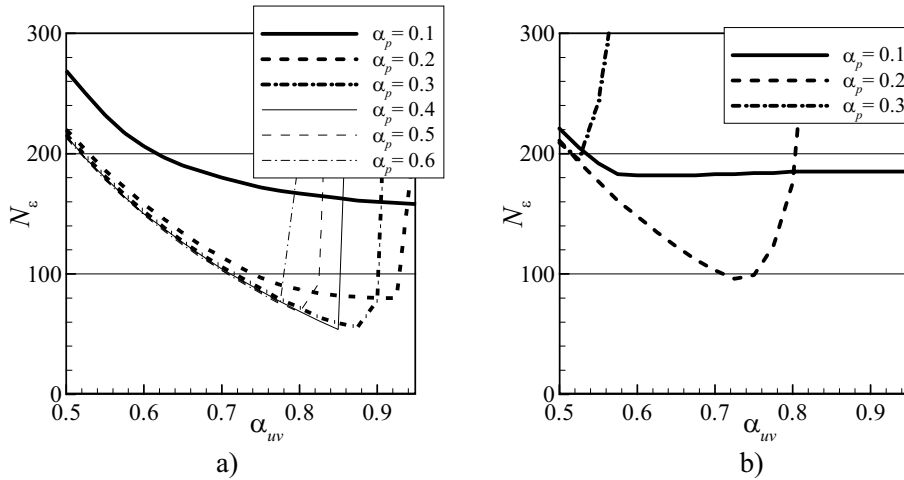Fig. 9. *A part of the computational grid for the curved-channel problem a) FVM, b) CAFFA*

Fig. 10. *Number of outer iterations required to reduce the residual levels to $\varepsilon = 10^{-6}$ for the curved-channel problem (UDS) a) FVM, b) CAFFA*

Fig. 8 shows the calculation domain and the stream-lines for this problem. Obviously, the final flow pattern is significantly different from the one that can be reasonably guessed at the beginning of the calculation.

Fig. 9 shows the part of the calculation area discretized with a locally orthogonal grid for the FVM and a structured grid for the CAFFA codes. The grid for the CAFFA code is non-orthogonal, and partially smoothed in the corners. In the straight parts of the channel this grid is orthogonal. The grid for the FVM code has 1180 finite volumes and the grid dimensions for the CAFFA code are 20×60 finite volumes. The uniform profile of the normal velocity v_n is given at the inlet. At the outlet boundary, the standard assumption of a zero velocity gradient is applied. The other boundaries are impermeable walls. The Reynolds number based on the normal velocity v_n and the inlet width a is Re $= \rho v_n \cdot a/\mu = 200$.

Fig. 10 shows N_ε for the SIMPLE algorithm on a locally orthogonal grid. The range of good values of the under-relaxation factors is wider than in the case of the non-orthogonal grid. For the non-orthogonal grid, N_ε increases considerably for small changes of the under-relaxation factors with respect to their optimum values.

Fig. 11 shows the convergence histories for two methods for a corresponding optimum combination of under-relaxation factors by using the UDS and the CDS. The advantage of the method on the locally orthogonal grid is obvious. The effects of the deferred correction approach in the CDS are superimposed on the effects of the grid's non-orthogonality.
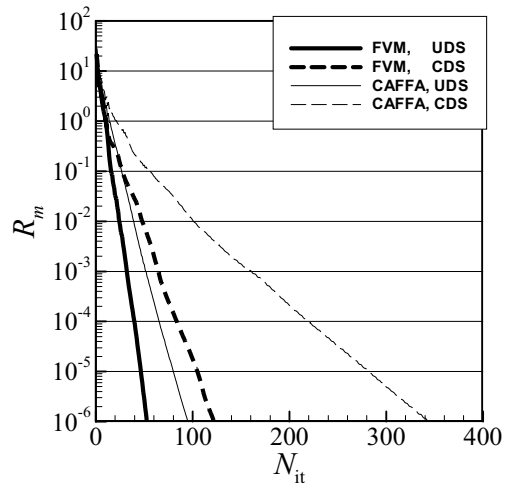

Fig. 11. *Convergence histories for the SIMPLE algorithm in the FVM and CAFFA codes for the curved-channel problem (UDS and CDS)*

3 CONCLUSIONS

From the comparison of the two methods in the selected test problems, the following conclusions can be drawn:
1) The results obtained by the FVM and CAFFA codes are nearly the same when both grids are orthogonal.
2) The method on a locally orthogonal grid implemented in the FVM code requires a smaller number of iterations than the method on a non-orthogonal grid implemented in the CAFFA code, when using corresponding optimum combinations of under-relaxation factors.

3) The range of under-relaxation factors for which the method converges is narrowing with the increase of the grid's non-orthogonality. This is a serious drawback, if we know that the optimum values of the under-relaxation factors are not known in advance, and that they take different values from problem to problem.

4) The application of the CDS based on the deferred correction approach increases the required number of iterations. This effect is superimposed on the effects of the grid's non-orthogonality.

4 LITERATURE

[1] Caretto, L.S., A.D. Gosman, S.V. Patankar und D.B. Spalding (1972) Two calculation procedures for steady, three-dimensional flows with recirculation. *Proceedings of Third International Conference on Numerical Methods in Fluid Dynamics*, Paris.

[2] Patankar, S.V., D.B. Spalding (1972) A calculation procedure for heat, mass, and momentum transfer in three dimensional parabolic flows. *Int. J. Heat Mass Transfer*, 15(1972), pp. 1787-1806.

[3] Rhie, C.M., W.L. Chow (1983) A numerical study of the turbulent flow past an isolated airfoil with trailing edge separation. *AIAA J.*, 21(1983), pp. 1525-1532.

[4] Ferzinger, J. H., M. Perić (1996) Computational methods for fluid dynamics. *Springer-Verlag*, New York.

[5] Džijan, I. (2004) Numerical method for fluid flow analysis on unstructured grid (in Croatian), PhD. Thesis. *University of Zagreb*, *Faculty of Mechanical Engineering and Naval Architecture,* Zagreb.

[6] Patankar, S.V. (1980) Numerical heat transfer and fluid flow. *McGraw-Hill*, New York.

[7] Perić, M. (1990) Analysis of pressure-velocity coupling on nonorthogonal grids. *Numerical Heat Transfer*, Part B; 17(1990), pp 63-82.

Authors' Addresses:
Doc. Dr. Ivo Džijan
Prof. Dr. Zdravko Virag
Dr. Hrvoje Kozmar
University of Zagreb
Faculty of Mechanical Engineering and
Naval Architecture
I. Lučića 5
HR-10000 Zagreb, Croatia
ivo.dzijan@fsb.hr
zdravko.virag@fsb.hr
hrvoje.kozmar@fsb.hr